PHYSICAL REVIEW B

CONDENSED MATTER

THIRD SERIES, VOLUME 45, NUMBER 9 1 MARCH 1992-I

Stimulated-emission cross sections and nonradiative relaxation of the $^5L_{6'}$ state of trivalent americium in fluorozirconate glass

Mark C. Williams and R. T. Brundage

Department of Physics and Astronomy, Macalester College, St. Paul, Minnesota 55105-1899

(Received 21 June 1991; revised manuscript received 3 September 1991)

The stimulated-emission cross section and nonradiative decay of the $^5L_{6'}$ state of trivalent americium in a fluorozirconate glass is analyzed as a function of temperature from 100 to 300 K. The emission cross section is calculated using the analysis of McCumber [D. E. McCumber, Phys. Rev. **134**, A299 (1964)] and compared to the observed fluorescence spectrum. Nonradiative rates are determined from the observed lifetimes and the calculated radiative rates, and compared to those reported for lanthanide ions in similar hosts.

I. INTRODUCTION

The study of the optical properties of actinide ions is important because of the potential for new optical devices and to test theories of optical emission and absorption of lanthanide ions. The actinide elements each have a lanthanide chemical analog, and this allows us to make direct comparisons between the observed behavior of $5f$-$5f$ actinide transitions and the predictions of theories developed for the $4f$-$4f$ transitions of lanthanide ions. This may aid in the development of accurate models for radiative[1-4] and nonradiative[5,6] decay of excited f-electron states.

Stimulated-emission cross sections are often hard to obtain, because of the difficulty in measuring absolute radiative emission rates. It is possible to obtain values for the emission cross section from the absorption spectrum, but it is necessary to take into account the thermal distribution of ions in both the excited and ground states.[7-9] Once the radiative rates are calculated, nonradiative rates can be inferred from the difference between the calculated and observed decay rates.

We have studied the absorption and fluorescence properties of Am^{3+} in fluorozirconate glass[10] as part of an ongoing study of actinide ions in glasses. The lanthanide analog of americium is europium, which is widely used as a fluorescent impurity.[11] The $J'=0$ ground state of Am^{3+} and Eu^{3+} leads to selection rules that make them interesting test cases for theories of optical transitions between f-electron states,[1-3,12] and also simplifies the analysis of the spectra. The prime on J indicates that intermediate coupling wave functions must be used, and that the states are labeled by the Russell-Saunders component that makes the dominant contribution to the wave function.

We have analyzed the absorption and fluorescence spectrum of the $^5L_{6'}$-$^7F_{0'}$ transition of Am^{3+} in a fluorozirconate glass as a function of temperature and calculated values for the stimulated-emission cross section. This allows us to determine the radiative and nonradiative decay rates of the $^5L_{6'}$ state and compare them with experimentally measured fluorescence lifetimes. We compare the nonradiative rate with the reported rates for lanthanide ions in fluorozirconate glasses.

II. THEORY AND BACKGROUND

The relationship between absorption and stimulated-emission cross sections is often calculated using the Einstein A and B coefficients, which were originally developed for a two-level system. However, in a multilevel system the oscillator strength of each component may not be the same and the states may not be equally populated. If this is the case, the Einstein relationship fails to predict the correct cross section.

In this case, however, the cross sections are still quantitatively related. An analysis developed by McCumber[7] and Nuporent[8] and generalized by Band and Heller[9] gives the relationship between the absorption cross section $\sigma_a(\nu)$ and the stimulated-emission cross section $\sigma_e(\nu)$ as

$$\sigma_e(\nu)=\sigma_a(\nu)\exp\{[\mu(T)-h\nu]/kT\}\ , \tag{1}$$

where $\mu(T)$ is the temperature-dependent "chemical potential" and the other variables have their usual meanings. This equation applies much more generally than the Einstein relation, since the only requirement of this relationship is that the ground and excited states are each in thermal equilibrium with the host, while not in equilibrium with each other.

The temperature dependence of $\mu(T)$ can be described

using the equation[8]

$$\frac{N_1}{N_2} = \exp[\mu(T)/kT] , \tag{2}$$

where N_1 and N_2 are the ground- and excited-state populations, respectively. This analysis has been applied to transition-metal[13] and lanthanide[14] ions in solids.

After obtaining values for the stimulated-emission cross section, it is possible to calculate the radiative decay rate of the transition through the relation

$$W_r = \frac{8\pi n^2}{c^2} \int \nu^2 \sigma_e(\nu) d\nu , \tag{3}$$

where W_r is the radiative rate and n is the refractive index. If the cross sections for all of the transitions from a state are known, their sum gives the total radiative rate. The inverse of the total radiative rate gives the radiative lifetime of the state. Alternatively, if the branching ratio of a transition rate to the total radiative rate is known, that transition rate can be used to calculate the radiative lifetime.

The nonradiative decay rate can then be calculated from the measured lifetime, using

$$\frac{1}{\tau} = W_r + W_{\rm nr} , \tag{4}$$

where τ is the observed lifetime of the excited state and $W_{\rm nr}$ is the nonradiative rate. Nonradiative rates determined at different temperatures can be compared with models used to describe the temperature dependence of nonradiative decay.

The temperature dependence of nonradiative decay of rare earths in solids can be described using[5]

$$W_{\rm nr} = Ce^{-a\Delta E}[n(\hbar\omega, T)+1]^p , \tag{5}$$

where $W_{\rm nr}$ represents the nonradiative decay rate, ΔE is the energy gap to the next lower state, p is the number of phonons required for that transition, and the two parameters C and a are characteristic of the material. The Bose-Einstein distribution $n(\hbar\omega, T)$ is evaluated for phonons of energy $\hbar\omega = \Delta E/p$ at temperature T. The phonon energy $\hbar\omega$ is that of the highest-energy phonon available in the host.

III. EXPERIMENTAL RESULTS AND ANALYSIS

The procedure for producing samples is given in Ref. 10. The host glass composition was 53% ZrF_4, 20% BaF_2, 4% LaF_3, 3% AlF_3, and 20% NaF_3 in mole percent. The sample used in this study has a number density of americium ions of 3.8×10^{18} cm^{-3}. The sample was cooled in a closed cycle helium refrigerator (RMC-Cryosystems model 22 CH). A grazing-incidence oscillator-amplifier dye laser pumped by a Molectron UV24 Nitrogen laser was used to excite the sample. The fluorescence intensity was measured using a cooled Hamamatsu R 649S (S-20 response) photomultiplier. The spectra were measured with a 1-m-focal-length Jarrell-Ash Czerny-Turner scanning spectrometer with a resolution of approximately 1 nm.

The signal was analyzed with a photon-counting system (Stanford Research Systems SR440 preamp and SR400 gated photon counter) for fluorescence spectra and a digitizing oscilloscope (Hewlett Packard 54200A) for fluorescence decays. The absorption cross section was measured using the same equipment with a tungsten filament lamp as a light source and a Keithley model 485 picoammeter to measure the signal. Absorption and reference spectra were taken separately. All signals were stored directly to computer files. Signal-to-noise ratios in the measured absorption spectrum were typically 25, and were limited by the stability of the lamp.

The measured absorption and fluorescence of the $^5L_{6'}$-$^7F_{0'}$ transition as a function of temperature is given in Fig. 1. The absorption spectrum is independent of temperature from 15 to 300 K, as expected for a system with a singlet ground state. At low temperature the fluorescence is at its lowest energy, which represents the transition from the lowest-energy Stark components of the excited-state manifold to the ground state. As the temperature is raised, the fluorescence curve begins to shift to higher energy, showing the thermal population of the higher Stark components of the excited-state manifold.

In order to obtain the stimulated-emission cross section from the absorption cross section through Eq. (1) we need to obtain values for $\mu(T)$. The ratio of $^7F_{0'}$ to $^5L_{6'}$ populations is given by

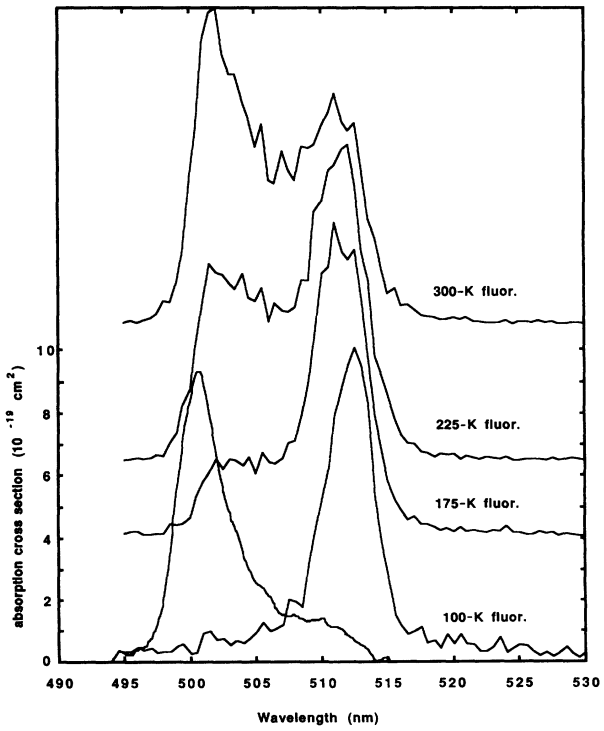

FIG. 1. Absorption spectrum at 15 K and fluorescence spectra at several temperatures. The curves are scaled so the peak heights are equal. The fluorescence spectra were taken with the photon counter gate set 50 μs wide and a delay of 5 μs from the laser pulse, and excited at approximately 465 nm.

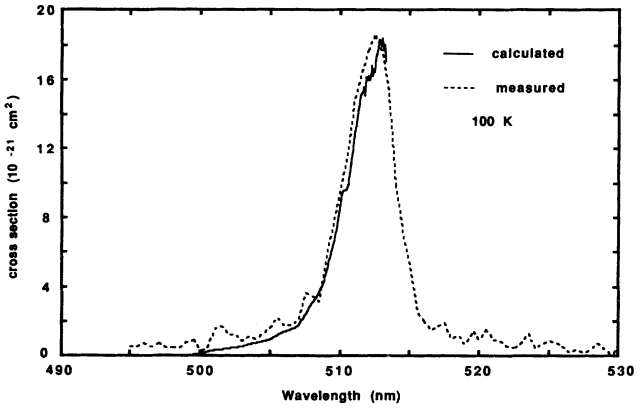

FIG. 2. Calculated stimulated-emission cross section and scaled fluorescence spectrum at 100 K.

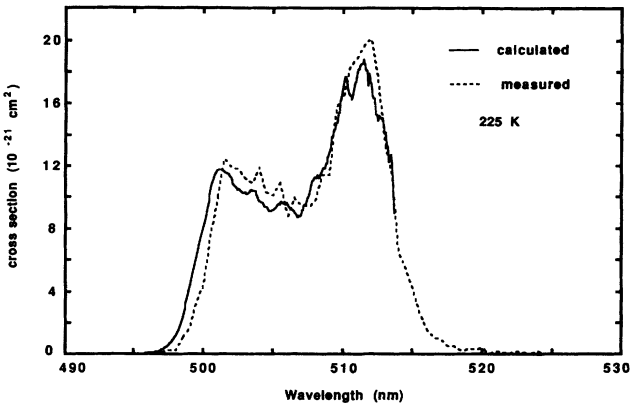

FIG. 4. Calculated stimulated-emission cross section and scaled fluorescence spectrum at 225 K.

$$\frac{N_1}{N_2}=\frac{\exp(E_0/kT)}{1+\sum_{j=2}^{13}\exp(-E_j/kT)}\,, \tag{6}$$

where E_0 is the separation between the lowest component of the excited-state manifold and the singlet ground state, given by the low-temperature fluorescence, and E_j is the separation between the jth component of the excited-state manifold and the lowest component of the manifold.[14] This equation requires detailed knowledge of the electronic structure, including knowledge of the separation between each component of the manifold. This information is not available because of the inhomogeneous broadening in the host, which causes overlap of the Stark components. The equation can be evaluated if one makes the approximation that all of the components are equally spaced. We obtained a value for the total width of the manifold of 660 cm^{-1} and a value for E_0 of 19 445 cm^{-1} from the spectra in Fig. 1. The separation between Stark components is taken to be this width divided by the number of individual separations. We then evaluated Eq. (6) at the temperatures illustrated in Fig. 1 and calculated $\mu(T)$ from Eq. (2).

We then used Eq. (1) to calculate the emission cross section from the absorption cross section. Figures 2–5 show the calculated cross sections and the measured fluorescence spectra. The calculated curves are incomplete because, due to the exponent in Eq. (1), the noise in the absorption data is greatly amplified at energies approaching $\mu(T)$.

To get the emission cross section over the entire range of fluorescence, the fluorescence data was scaled using the emission cross sections calculated from Eq. (1). We integrated the calculated emission cross sections over the limited range of wavelengths shown in Figs. 2–5. The fluorescence data were scaled so that their integral over the same range equaled that of the calculated cross sections. The scaled fluorescence data can then be integrated over the entire emission range to give the total stimulated-emission cross section. The scaled fluorescence data is also shown in Figs. 2–5.

The values obtained from the scaling of the fluorescence data were used to calculate the radiative rate as a function of temperature using Eq. (3). The total radiative rate was calculated using a branching ratio of 65%.[15]

These radiative rates can be compared to the observed fluorescence lifetimes. The decay of the fluorescence is

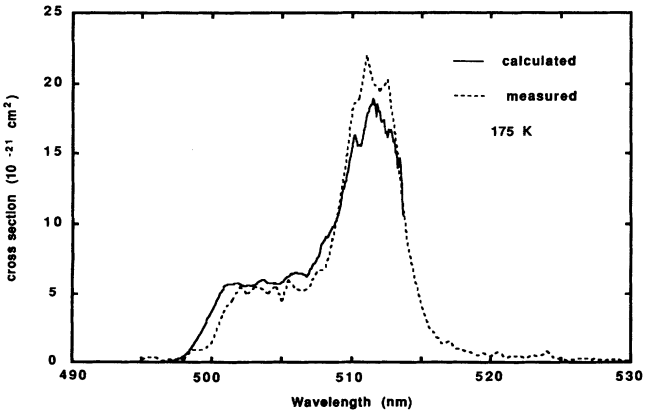

FIG. 3. Calculated stimulated-emission cross section and scaled fluorescence spectrum at 175 K.

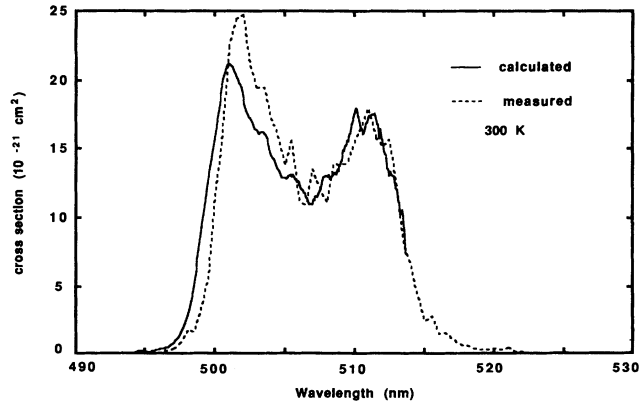

FIG. 5. Calculated stimulated-emission cross section and scaled fluorescence spectrum at 300 K.

TABLE I. Temperature-dependent nonradiative decay rates calculated from Eq. (7), radiative decay rates from the calculated stimulated-emission cross section, the resultant total decay rates and lifetimes, and the experimentally measured lifetimes.

T (K)	W_{nr} (10^3 s^{-1})	W_r (10^3 s^{-1})	$W_{nr}+W_r$ (10^3 s^{-1})	τ_{calc} (μs)	τ_{meas} (μs)
100	63	4.2	67	15.0[a]	15.0
175	67	6.0	73	13.6	13.2
225	75	7.5	83	12.1	11.0
300	93	9.6	103	9.7	9.2

[a]Measured lifetime and calculated radiative rate at 100 K used to determine low-temperature nonradiative rate.

nonexponential.[10] The decay rate was determined using the signal from 2.5 to 25 μs after the laser pulse, which is very nearly a single exponential. We used the experimentally measured decay rate and the calculated radiative rate at 100 K to estimate the low-temperature nonradiative rate $W_{nr}(0)$ of 63 000 s^{-1}. We then calculated the nonradiative rate at higher temperatures using the equation

$$W_{nr}(T)=W_{nr}(0)[n(\hbar\omega,T)+1]^p \quad (7)$$

with $\hbar\omega=500$ cm^{-1} and $\Delta E=2230$ cm^{-1}, leading to $p=4.5$. The calculated radiative and nonradiative rates are summarized in Table I, along with the observed fluorescence lifetimes.

IV. DISCUSSION

The fact that the fluorescence of the $^5L_{6'}\rightarrow{}^7F_{0'}$ transition is shifted down in energy from the absorption curve helps to explain a discrepancy in the calculation of the energies of low-lying states of Am^{3+} in ZBLAN found in Ref. 10. Table II contains the transitions discussed in that paper with three corrections, all of which used the $^5L_{6'}$-$^7F_{0'}$ transition to calculate the energies of the terminal states. The earlier study used the absorption spectrum to determine the energy of this transition, because the fluorescence was excited by pumping the $^5L_{6'}$ state directly and scattered laser light prevented the observation of the resonant fluorescence. The energy of the low-temperature $^5L_{6'}$-$^7F_{0'}$ fluorescence peak gives much better agreement for the energies of the $^7F_{1'}$ and $^7F_{2'}$ states with the values determined from the $^5D_{1'}$ fluorescence.

We also found that both the radiative and nonradiative decay rates are temperature dependent. Using the calculated total radiative rates, a constant branching ratio of 65%, and the calculated nonradiative rates we were able to generate values for the lifetime of the excited state that are in excellent agreement with the experimentally measured lifetimes.

The decay rates discussed above are very important in calculating the potential of a transition for laser applications. We found that the nonradiative rates are more than an order of magnitude greater than the radiative rates. This may help to explain the unsuccessful attempts to make americium lase.[16] The nonuniform population of the Stark components means that the absorption spectrum does not reflect the radiative rate at room temperature. It is a coincidence that in this case the observed lifetime of ~ 10 μs agrees roughly with the radiative lifetime calculated from the absorption spectrum using the Einstein approximation, 60 μs. Successful laser action in americium will require a host with either smaller crystal-field splitting or rearrangement of the crystal-field so that the stronger transitions occur at lower energy relative to the weak ones.

The energy-gap law of Eq. (5) has been thoroughly studied for many lanthanide transitions. It is found that $C=1.88\times10^{10}$ s^{-1} and $a=5.77\times10^{-3}$ cm for fluorozirconate glasses,[17] which gives a value for $W_{nr}(0)$ of 48 000 s^{-1} for $\hbar\omega=500$ cm^{-1} and $\Delta E=2230$ cm^{-1}. The value for americium, 63 000 s^{-1}, is larger. This is consistent with the idea that actinides have a stronger electron-phonon coupling than the lanthanides. Studies of other transitions between $5f$ states will allow determination of the C and a parameters for actinides in fluorozirconate glasses, which will be useful in evaluating the possibility of actinide-based luminescent devices.

V. CONCLUSION

We have shown the ability of the analysis developed by McCumber to predict the temperature dependence of actinide fluorescence using the approximation that the Stark components of the excited state are equally spaced. We obtained values for the stimulated-emission cross section as a function of temperature using the experimentally measured absorption cross section and fluorescence

TABLE II. Energies of electronic states of Am^{3+}.

State	Transition	ZBLAN:AmF_3 Energy (cm^{-1})	$AmCl_3$, Ref. 18 Energy (cm^{-1})
$^7F_{0'}$		0	0
$^7F_{1'}$	$^5D_{1'}\rightarrow{}^7F_{1'}$	17 240 − 14 540 = 2 700	2 720
	$^5L_{6'}\rightarrow{}^7F_{1'}$	19 470 − 16 720 = 2 750	
$^7F_{2'}$	$^5D_{1'}\rightarrow{}^7F_{2'}$	17 240 − 12 030 = 5 210	5 308
	$^5L_{6'}\rightarrow{}^7F_{2'}$	19 470 − 14 190 = 5 280	
$^5D_{1'}$	$^5D_{1'}\rightarrow{}^7F_{0'}$	17 240 − 0 = 17 240	16 906[a]
$^5L_{6'}$	$^5L_{6'}\rightarrow{}^7F_{0'}$	19 170 − 0 = 19 470	19 627

[a]The energy level for state $^5D_{1'}$ reported in Ref. 19 was observed in AmI_3.

spectra. From the calculated cross section we obtained values for the radiative decay rates as a function of temperature which, when combined with calculated nonradiative decay rates, correctly predict the measured lifetimes. The calculated nonradiative rates of Am^{3+} are greater than expected for a lanthanide ion in the same host. The radiative rate increases faster than the nonradiative rate with increasing temperature, so the quantum efficiency actually increases as a function of temperature, at least up to room temperature. We have carried out preliminary experiments that confirm this unusual behavior. We find that the integrated fluorescence intensity increases by a factor of 1.2 when the temperature changes from 100 to 300 K, in reasonable agreement with the value of 1.4 obtained by taking the ratio of calculated radiative and total decay rates for each temperature. We plan to continue to investigate this behavior in this sample as well as in other glass hosts.

ACKNOWLEDGMENTS

We are pleased to acknowledge the assistance of William T. Carnall, James, V. Beitz, and Clayton Williams of the Argonne National Laboratory Chemistry Division in preparing and characterizing the samples. We are indebted to Martin Drexhage and his colleagues at Galileo Electro-Optics Corp. for providing updoped glass for the sample. Bill Miniscalco of GTE labs called our attention to the McCumber analysis. This research is supported by the National Science Foundation through Grant No. DMR 881-3333. One of us (R. T. B.) received partial support from Argonne National Laboratory Division of Educational Programs.

[1]B. R. Judd, Phys. Rev. **127**, 750 (1962).
[2]G. S. Ofelt, J. Chem. Phys. **37**, 511 (1962).
[3]R. D. Peacock, Struct. Bonding (Berlin) **22**, 83 (1975).
[4]G. W. Burdick, M. C. Downer, and D. K. Sardar, J. Chem. Phys. **91**, 1511 (1989).
[5]C. B. Layne, W. H. Lowdermilk, and M. J. Weber, Phys. Rev. B **16**, 10 (1977).
[6]M. F. H. Schuurmans and J. M. F. v. Dijk, Physica B+C **123B**, 131 (1984).
[7]D. E. McCumber, Phys. Rev. **134**, A299 (1964).
[8]B. S. Neporent, Dokl. Akad. Nauk SSSR **119**, 682 (1958) [Sov. Phys. Dokl. **3**, 337 (1958)].
[9]Y. B. Band and D. F. Heller, Phys. Rev. A **38**, 1885 (1988).
[10]Rául W. Valenzuela and R. T. Brundage, J. Chem. Phys. **93**, 8469 (1990).
[11]H. G. Brittain in *Molecular Luminescence Spectroscopy: Methods and Applications—Part II,* edited by S. J. Schulman (Wiley, New York, 1988), pp. 401-459.
[12]T. R. Faulkner and F. S. Richardson, Mol. Phys. **35**, 1141 (1978).
[13]M. Sekita, Y. Miyazawa, and S. Kimura, J. Appl. Phys. **58**, 3658 (1985).
[14]W. J. Miniscalco and R. S. Quimby, Opt. Lett. **16**, 257 (1991).
[15]R. T. Brundage, Michelle M. Svatos, and Raitis Grinbergs, J. Chem. Phys. **95**, 7933 (1991).
[16]B. Finch and G. W. Clark, J. Phys. Chem. Solids **34**, 922 (1973).
[17]M. D. Shinn, W. A. Sibley, M. G. Drexhage, and R. N. Brown, Phys. Rev. B **27**, 6635 (1983).
[18]R. G. Pappalardo, W. T. Carnall, and P. R. Fields, J. Chem. Phys. **51**, 1182 (1969).